



# Endoplasmic reticulum stress and oxidative stress drive endothelial dysfunction induced by high selenium

Matshediso Zachariah<sup>1</sup> | Hatem Maamoun<sup>1</sup> | Larissa Milano<sup>1</sup> |  
Margaret P. Rayman<sup>2</sup> | Lisiane B. Meira<sup>1</sup> | Abdelali Agouni<sup>3</sup>

<sup>1</sup>Department of Clinical and Experimental Medicine, Faculty of Health and Medical Sciences, University of Surrey, Guildford, UK

<sup>2</sup>Department of Nutritional Sciences, Faculty of Health and Medical Sciences, University of Surrey, Guildford, UK

<sup>3</sup>Department of Pharmaceutical Sciences, College of Pharmacy, QU Health, Qatar University, Doha, Qatar

## Correspondence

Lisiane B. Meira, Department of Clinical and Experimental Medicine, Faculty of Health and Medical Sciences, University of Surrey, Guildford, UK.

Email: [l.meira@surrey.ac.uk](mailto:l.meira@surrey.ac.uk)

Abdelali Agouni, Department of Pharmaceutical Sciences, College of Pharmacy, QU Health, Qatar University, P. O. Box 2713, Doha, Qatar.

Email: [aagouni@qu.edu.qa](mailto:aagouni@qu.edu.qa)

## Present address

Matshediso Zachariah, Faculty of Health Sciences, School of Allied Health Professions, University of Botswana, Gaborone, Botswana

Hatem Maamoun, Department of Medical Biochemistry and Molecular Biology, Faculty of Medicine, Ain Shams University, Abbaseyya, Cairo11591Egypt

Larissa Milano, Genome Stability Laboratory, CHU de Québec Research Center, HDQ Pavilion, Oncology Division, 9 McMafrhon, Québec, QC, Canada.

## Funding information

Qatar National Research Fund, Grant/Award Number: UREP24-016-3-004; Qatar National Library; Royal Society, Grant/Award Number: RG120480; Qatar University, Grant/Award Number: QU CG-CPH-20/21-3

## Abstract

Selenium is an essential trace element important for human health. A balanced intake is, however, crucial to maximize the health benefits of selenium. At physiological concentrations, selenium mediates antioxidant, anti-inflammatory, and pro-survival actions. However, supra-nutritional selenium intake was associated with increased diabetes risk leading potentially to endothelial dysfunction, the initiating step in atherosclerosis. High selenium causes apoptosis in cancer cells via endoplasmic reticulum (ER) stress, a mechanism also implicated in endothelial dysfunction. Nonetheless, whether ER stress drives selenium-induced endothelial dysfunction, remains unknown. Here, we investigated the effects of increasing concentrations of selenium on endothelial cells. High selenite reduced nitric oxide bioavailability and impaired angiogenesis. High selenite also induced ER stress, increased reactive oxygen species (ROS) production, and apoptosis. Pretreatment with the chemical chaperone, 4-phenylbutyrate, prevented the toxic effects of selenium. Our findings support a model where high selenite leads to endothelial dysfunction through activation of ER stress and increased ROS production. These results highlight the importance of tailoring selenium supplementation to achieve maximal health benefits and suggest that prophylactic use of selenium supplements as antioxidants may entail risk.

## KEYWORDS

apoptosis, endoplasmic-reticulum stress, endothelial dysfunction, oxidative stress, selenium

This is an open access article under the terms of the Creative Commons Attribution License, which permits use, distribution and reproduction in any medium, provided the original work is properly cited.

© 2020 The Authors. *Journal of Cellular Physiology* published by Wiley Periodicals LLC

## 1 | INTRODUCTION

Cardiovascular disease is a major public health concern accounting for around 31% of all global deaths and representing an important economic burden on healthcare systems worldwide (WHO, 2017). Cardiovascular disease is initiated by dysfunction of the endothelium, a single layer of endothelial cells lining the inner surface of all blood vessels that regulate vascular homeostasis (Levick, 2003). Endothelial dysfunction is a major risk factor for cardiovascular disease and is mainly characterized by reduced bioavailability of nitric oxide (NO), the main vasodilator generated by endothelial NO synthase (eNOS; Cunningham & Gotlieb, 2005; Hermann et al., 2006; Levick, 2003).

Vascular homeostasis is maintained by an equilibrium between the generation of reactive oxygen species (ROS) and NO production. Indeed, cardiovascular risk factors such as dyslipidemia, high blood pressure, and smoking disrupt this equilibrium by enhancing ROS production and decreasing endothelial NO release leading eventually to impaired NO bioavailability and hence endothelial cell dysfunction (Abdelsalam et al., 2019; Dinh et al., 2014; Pennathur & Heinecke, 2007). Moreover, pivotal molecular events in the process of atherogenesis such as lipoxidation and activation of endothelial cells, are aided by vascular ROS and curbed by endothelial NO. This is important because increased ROS production leads to eNOS uncoupling, which switches to catalyzing the production of superoxide ( $O_2^-$ ) at the expense of NO, and oxidative inactivation of NO by  $O_2^-$ , thereby further reducing NO bioavailability and impairing vascular function (Incalza et al., 2018).

Recently, endoplasmic reticulum (ER) stress was shown to play a key role in endothelial dysfunction (Choi et al., 2016; Galán et al., 2014; Maamoun et al., 2017). Upon increased demand for protein synthesis, accumulation of misfolded or unfolded proteins triggers the cytoprotective unfolded protein response (UPR; Hetz, 2012; Schwarz & Blower, 2016). Three ER transmembrane proteins coordinate the UPR: protein kinase RNA-like endoplasmic reticulum kinase (PERK), inositol requiring enzyme-1 $\alpha$  (IRE-1 $\alpha$ ), and activation transcription factor-6 (ATF-6), which are maintained inactive through their interaction with chaperone binding immunoglobulin protein (BiP). BiP dissociates from these effectors upon accumulation of unfolded proteins, resulting in their activation. UPR activates parallel pathways to up-regulate protein-folding machinery to decrease the burden of unfolded proteins on the ER (Abdelsalam et al., 2019; Hetz, 2012; Schroder & Kaufman, 2005; M. Wang & Kaufman, 2014). Prolonged activation of UPR leads to ER stress response and is associated with the activation of inflammatory and apoptotic signals such as C/EBP homologous protein (CHOP) and ATF-4 (Cnop et al., 2012; Sozen et al., 2015; M. Wang & Kaufman, 2014).

ER stress was shown to play a critical role in endothelial cell death and inflammation in several models of diabetes (Chen et al., 2012; Galan et al., 2012; Lenna et al., 2014). Mice injected with streptozotocin (STZ) to induce diabetes exhibited endothelial cell dysfunction and impaired angiogenesis in a mechanism involving

ER stress and the activation of ATF-4 transcription (Chen et al., 2012). It has also been reported that injection of mice with STZ caused an abnormal elevation in the activity of epidermal growth factor receptor (EGFR) tyrosine kinase accompanied by the induction of ER stress response and microvascular dysfunction (Galan et al., 2012). Besides diabetes, other major risk factors of cardiovascular disease, including hyperglycemia (Werstuck et al., 2006), hyperhomocysteinemia (Werstuck et al., 2001), and obesity (Agouni et al., 2011; Delibegovic et al., 2009; Ozcan et al., 2004) have also been shown to induce the ER stress response, indicating a focal role for ER stress in the process of atherogenesis. In agreement with this, it has been reported that markers of ER stress were observed at all steps of the atherogenesis process (Zhou et al., 2005).

Selenium, available through the diet, is an essential trace element required for the synthesis of selenoproteins which incorporate selenium in their structure as selenocysteine (Burk & Hill, 2015). Selenomethionine (SeMet) is the commonest form of selenium found in foods including offal, seafood, meat, and cereals; sodium selenite is a commonly used selenium supplement (Rayman, 2012). Given the antioxidant activities of a number of the selenoproteins, selenium has been used to mitigate against oxidative stress in multiple pathologies including cancers, degenerative nerve diseases, diabetes, and cardiovascular disorders (Pillai et al., 2014; Rayman, 2012). However, at higher concentrations, selenium use has been associated with oxidative stress and cell dysfunction (Ip, 1998; Labunskyy et al., 2011; Steinbrenner et al., 2011). In fact, much evidence from in vivo and in vitro reports indicates that excessively low and high selenium concentrations are associated with a higher risk of disease, including diabetes and cardiovascular disease (Bleys et al., 2007; Bleys, Navas-Acien, & Guallar, 2008; Bleys, Navas-Acien, Stranges, et al., 2008; Labunskyy et al., 2011; Rayman, 2012; Rocourt & Cheng, 2013). This U-shaped relationship between selenium status and optimal health suggests a complex role for selenium in physiology (Bleys, Navas-Acien, Stranges, et al., 2008; Ibrahim et al., 2019; Rayman, 2020). Although a few observational studies found an inverse association between selenium status and cardiovascular risk, post hoc analysis of the Nutritional Prevention of Cancer trial found that long-term supplementation with selenium (200  $\mu$ g/day) increased type-2 diabetes risk (Stranges et al., 2007) a condition intimately associated with endothelial cell dysfunction and cardiovascular complications (Maamoun, Benameur, et al., 2019). In this context, it is crucial to delineate the role of selenium in endothelial cell dysfunction and the molecular or cellular mechanisms underlying these paradoxical effects.

We hypothesized that high selenium concentrations may lead to endothelial cell dysfunction via the induction of ER stress. To address this, we investigated the effects of exposing cultured endothelial cells to physiological and supra-physiological concentrations of selenium on angiogenic capacity, a key feature of endothelial cell function. Furthermore, we assessed the role of ER stress-mediated cell death and oxidative stress in this process.

## 2 | MATERIALS AND METHODS

### 2.1 | Cells and cell maintenance

EA.hy926 endothelial cell line, obtained from the American Type Culture Collection (cat #CRL-2922; ATCC), was maintained in high glucose (4.5 g/L) Dulbecco's modified Eagle's medium supplemented with 10% fetal bovine serum (cat #F9665), L-glutamine (2 mmol/L; cat #G7513) and penicillin (10,000 units) and 10 mg streptomycin per ml (cat #P9333; all from Sigma-Aldrich).

Primary human umbilical vein endothelial cells (HUVECs; cat #C-006-5C and #C-015-10C; Life Technologies) were maintained in M200 media (cat #M200500; Gibco™, Life Technologies) supplemented with low serum growth supplement (LSGS; cat #S-003-10; Gibco™, Life Technologies). Cells were maintained at 37°C in a 95% humidified atmosphere with 5% CO<sub>2</sub>. HUVECs were used in experiments up to passage 6. Sodium selenite (cat #S5261; Sigma-Aldrich) was used as a source of selenium for experiments, unless otherwise specified.

### 2.2 | 3-(4,5-Dimethylthiazol-2-yl)-2,5-diphenyltetrazolium bromide (MTT) assay viability assay

Cellular viability was measured using the tetrazolium salt MTT assay (cat #475989; Sigma-Aldrich). EA.hy926 cells were cultured in 96-well plates ( $5 \times 10^4$  cells/well) and incubated with sodium selenite (0, 0.5, 5, 10, 20 μM; cat #S5261), sodium selenate (cat #8295; 0, 0.5, 5, 10, 20 μM) or seleno-L-methionine (SelMet; cat #S3132; 0, 0.5, 5, 10, 15, 20 μM) for 24 h before MTT assay (all from Sigma-Aldrich). The assay was performed four independent times (16 technical replicates per condition and experiment), and cell viability was presented as the proportion (%) of live cells compared to the control group (untreated cells).

### 2.3 | Matrigel angiogenesis assay

HUVECs were cultured in six-well plates ( $2 \times 10^5$  cells/well) and left overnight to attach. Following this, sodium selenite was added for a further 24 h in combination or not with the chemical chaperone, sodium 4-phenylbutyrate (PBA, 20 mM; cat #P21005; Sigma-Aldrich) or PERK inhibitor (GSK2606414, 10 μM; cat #516535; Calbiochem). Following treatments, cells were seeded in triplicate on 24-well culture plates coated with Matrigel (BD Bioscience) at the density of  $1 \times 10^5$  cells/well. Untreated cells, maintained in LSGS-supplemented M200 medium, were considered to be a negative control, while cells incubated in complete M200 medium supplemented with human recombinant vascular endothelial growth factor (VEGF; 50 ng/ml; Life Technologies) were used as positive controls. After 6 h of incubation, tube-like structures were imaged using a phase-contrast

Olympus CX21 inverted microscope fitted with a digital camera at  $\times 40$  and  $\times 100$  magnification (Olympus Europa). Tube-like structure formation was analyzed with the Angiogenesis Analyzer plug-in on ImageJ. Tube lengths were counted in five blind fields per well, averaged, normalized to control, and then compared across the experimental groups. Experiments were conducted four independent times.

### 2.4 | Indirect assessment of NO by Griess assay

HUVECs were cultured in 96-well plates at a density of  $1 \times 10^4$  cells/well and left to attach overnight, before treatment with sodium selenite in combination or not with PBA (20 mM) for 24 h. The Griess reagent was used to determine the concentration of nitrite/nitrate, stable NO degradation metabolites, which indirectly reflects the levels of NO according to the manufacturer's protocol (cat #ab234044; Abcam). The culture medium was harvested from treatment conditions and rapidly centrifuged to eliminate any detached cells or debris. Finally, nitrate and nitrite concentrations were determined by following the manufacturer's recommendations, and values extrapolated from a standard curve were used to determine the concentration of nitrite. The concentration of the nitrite formed was proportional to the amount of NO produced by the cells when measured at 548 nm.

### 2.5 | Measurement of ROS

We determined the effect of selenium on the generation of O<sub>2</sub><sup>-</sup>, the main ROS produced by the endothelium, using flow cytometry (FACS CANTO II; BD Bioscience) and the dihydroethidium (DHE; cat #12013; Sigma-Aldrich) dye, as described previously (Mostefai et al., 2008). Briefly, cells ( $2 \times 10^6$  cells/well) were treated with selenite in combination or not with PBA (20 mM) and incubated for 8 h, and then analyzed by flow cytometry. Hydrogen peroxide (100 μM; cat #95321; Sigma-Aldrich) was used as a positive control. Experiments were performed independently three times.

### 2.6 | mRNA expression analysis

After treatments, total RNA was extracted using the RNeasy mini kit (cat # 74104; Qiagen) according to the manufacturer's instructions. Genomic DNA was digested by DNAase I (cat #89836; Thermo Fisher Scientific). Then, first-strand cDNA was prepared from 1 μg of total RNA using a commercial kit (cat #K1621; Thermo Fisher Scientific) by following the manufacturer's recommendations. After this, mRNA expression of target genes was detected by real-time PCR in a 7500 PCR System from Applied Biosystems (Thermo Fisher Scientific). All experiments were performed with independent biological and technical triplicates. For data analyses, the comparative

$C_t$  method was used, and data are expressed as fold-change relative to the untreated control. The pairs of primers for human target genes were sourced from Primer bank and synthesized by Sigma-Aldrich. Human primer sequences used in the study are listed in Table 1.

## 2.7 | Western blot analysis

Following cell treatments, whole-cell lysates were collected using radioimmunoprecipitation assay (RIPA) lysis and extraction buffer. Equal quantities of proteins (10–20  $\mu$ g) were resolved on gradient sodium dodecyl sulfate-polyacrylamide gel electrophoresis gels (8–12%; Thermo Fisher Scientific). The following primary antibodies were used for immunoblotting: polyclonal rabbit anti-BiP (cat #3177; 1:500), monoclonal rabbit anti-phospho-eukaryotic translation initiation factor 2 $\alpha$  (119A11; cat #3597; eIF2 $\alpha$ ; SER51; 1:1000; Cell Signaling Technology®) and mouse anti- $\alpha$ -Tubulin (cat #ab7291; 1:5000; Abcam). After probing with primary antibodies, membranes were incubated with the following secondary antibodies; IRDye 680RD goat anti-rabbit IgG (cat #926-32211) and IRDye 800CW goat anti-mouse (cat #926-32210; 1:5000; Li-COR Biosciences). Immunoblots were imaged with an ODYSSEY®CLX infrared imaging system scanner (Li-COR Biosciences). The signal was then quantified using Image Studio software from Li-COR Biosciences.

## 2.8 | X-box binding protein 1 (XBP-1) splicing assay

*XBP-1u* (unspliced) and *XBP-1s* (spliced) transcripts were detected as described previously (Yoshida et al., 2001). We analyzed the splicing of *XBP-1* from cDNA using Go Taq® Green Master Mix (cat #M7822; Promega). The PCR amplification conditions were as follows: 94°C for 3'; followed by 35 cycles (94°C for 10", 65°C for 30", and 72°C for 30"); and finally, 10 min at 72°C. The following primer sequences were used for amplification: Forward 5'-CCTTGATGTTGAGAAC CAGG-3' and reverse 5'-GGGGCTTGGTATATATGTGG-3'. PCR amplification products were then resolved on an agarose gel (2.5%).

## 2.9 | Assessment of cell death

Cell death was assessed using an ApoScreen® Annexin V Apoptosis Kit (cat #10010-09; Cambridge Bioscience) following the manufacturer's instructions. In brief, cells were cultured in six-well plates at the density of  $2 \times 10^5$  cells/well overnight followed by sodium selenite treatment for 24 h in combination or not with PBA (20 mM; Sigma-Aldrich). Cells (20,000 cell/ml) were then labelled with Annexin V-PE dye. Cells were incubated for 15 min on ice, away from light, then 7-AAD dye was added with binding buffer according to the manufacturer's protocol. Following this, samples were immediately analyzed with BD FACSCanto™ II (BD Bioscience). Cells undergoing apoptosis were expressed as the percentage of total cells counted. A positive control was derived from cells treated for 3 h with Staurosporine (cat #S5921; 1  $\mu$ M; Sigma-Aldrich) whereas nontreated cells represent negative controls.

## 2.10 | Caspase 3/7 activity

Caspase activity was assessed with the Caspase-Glo® 3/7 assay (cat #G8090; Promega), according to the manufacturer's instructions. Cells were cultured in white-walled 96-well plates ( $1 \times 10^4$  cells/well) and treated with selenite for 24 h in the presence or absence of PBA (20 mM). A group of cells incubated with Staurosporine (1  $\mu$ M, 3 h) was considered as a positive control. Caspase 3/7 activity was assessed using a LUMIstar Omega® luminometer (BMG Labtech). Enzymatic activity is expressed as a percentage relative to the control.

## 2.11 | Statistical analysis

Results are expressed as mean  $\pm$  SEM or percentage  $\pm$  SEM, as appropriate. Statistical analysis was conducted with GraphPad Prism® 7.01e software using either one-way analysis of variance (ANOVA) or two-way ANOVA followed by Tukey's or Bonferroni multiple comparison post hoc tests, respectively. A  $p \leq .05$  was considered statistically significant.

**TABLE 1** Sequence of primers for the detection of mRNA of human genes studied in qPCR experiments

Target	Forward	Reverse
ATF-4	5'-CCCTTCACCTTCTTACAACTC-3'	5'-TGCCCAGCTCTAAACTAAAGGA-3'
BiP	5'-CATCACGCCGCTCTATGTCG-3'	5'-CGTCAAAGACCGTGTCTCG-3'
Caveolin-1	5'-GCGACCCTAAACACCTCAAC-3'	5'-ATGCCGTCAAACTGTGTGTC-3'
CHOP	5'-GAACGGCTCAAGCAGGAAATC-3'	5'-TTCACCATTCCGGTCAATCAGAG-3'
IL-6	5'-AAATTCGGTACATCCTCGACGG-3'	5'-GGAAGGTTTCAGTTGTTTTCTGC-3'
MCP-1	5'-CAGCCAGATGCAATCAATGCC-3'	5'-TGGAATCCTGAACCCACTTCT-3'
$\beta$ -Actin	5'-CATGTACGTTGCTATCCAGGC	5'-CTCCTTAATGTCACGCACGAT-3'

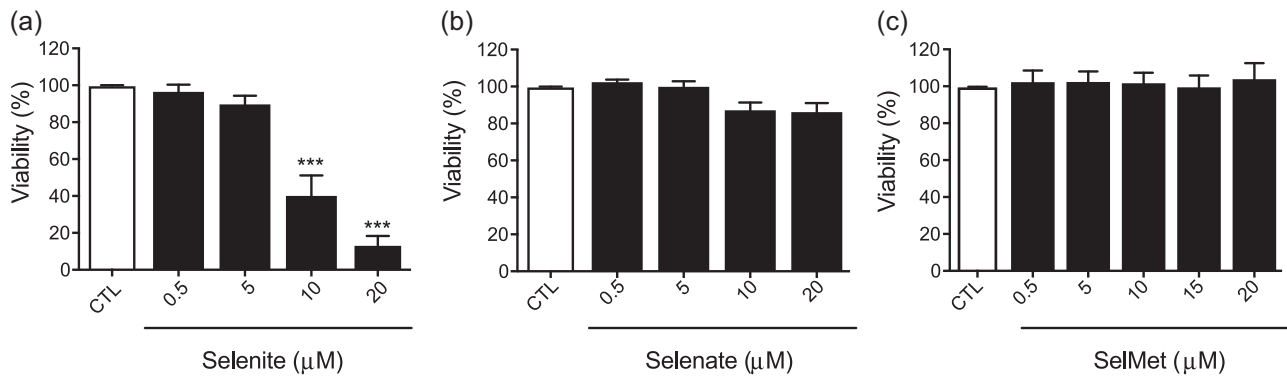


**FIGURE 1** The effects of selenium on endothelial cell viability. Cell viability expressed as a percentage of control (CTL) in EA.hy926 cells incubated with (a) sodium selenite, (b) sodium selenate, and (c) SelMet. Results are presented as mean  $\pm$  SEM and analyses were done by one-way analysis of variance followed with a Tukey's post hoc multiple comparison test;  $n = 4$ . \*\*\* $p < .001$  versus untreated group (CTL)

### 3 | RESULTS

#### 3.1 | High selenite concentrations reduced endothelial-cell viability

To determine the effect of selenium on endothelial cell viability, inorganic selenium supplements, sodium selenite, sodium selenate, and organic SelMet were used. The concentrations used ranged from a physiological concentration of  $0.5 \mu\text{M}$  (the optimal plasma concentration range for selenium is  $0.5$ – $1.5 \mu\text{M}$ ; Burk, 2002) to high concentrations of selenium of  $5$ ,  $10$ , and  $20 \mu\text{M}$  (Wu et al., 2005; Xiang et al., 2009). High concentrations of sodium selenite led to a significant reduction in cell viability after 24 h of exposure (Figure 1a). As depicted in Figure 1a, high concentrations of selenite, that is,  $10$  and  $20 \mu\text{M}$ , significantly reduced viable endothelial cells to 39% and 13%, respectively ( $p < .001$ ) compared to the untreated group. Other selenium compounds, selenate (Figure 1b) and SelMet (Figure 1c) did not affect cell viability at the concentrations tested. Thus, these results show that supra-physiological concentrations of sodium selenite, the inorganic selenium supplement that is also used in cancer therapy (Selenius et al., 2010) caused toxicity to endothelial cells.

#### 3.2 | High selenite concentrations activated the ER stress response in endothelial cells

We assessed next whether selenium-induced toxicity was associated with ER stress induction by examining signature ER stress markers, namely, phospho-eIF2 $\alpha$ , XBP-1 splicing, ATF-4, BiP, and CHOP. Figure 2 shows the results in cells incubated with various concentrations of selenite for 24 h. Sodium selenite at high concentrations induced an increase in mRNA expression of CHOP (Figure 2a) and ATF-4 (Figure 2b). In addition, increases in protein levels of BiP and the phosphorylation of eIF2 $\alpha$  (Ser51) caused by high concentrations of selenite were detected by western-blot analysis (Figure 2c). Finally, sodium selenite treatment at high concentrations

induced XBP-1 splicing (Figure 2d). Altogether, these data indicate that high concentrations of selenite activated ER stress response in endothelial cells.

The activation of ER stress caused by high concentrations of selenite was associated with a significant increase in mRNA expression of two inflammatory markers, the pro-inflammatory cytokine interleukin-6 (IL-6; Figure 3a) and monocyte chemoattractant protein-1 (MCP-1; Figure 3b), an important chemokine that facilitates migration and infiltration of monocytes, suggesting cellular inflammation. These data suggest a possible activation of inflammatory responses in cells exposed to high selenite concentration.

#### 3.3 | High selenite concentrations induced endothelial-cell dysfunction and impaired angiogenic capacity by reducing NO bioavailability in an ER-stress-dependent fashion

To determine whether ER stress induced by sodium selenite affects endothelial cell function, we used the tube-like structure-formation assay to assess the angiogenic ability of endothelial cells after treatment with sodium selenite. We found that the endothelial cell tube-like structure formation ability was reduced after treatment with high selenium concentrations (Figure 4a,b), with a marked decrease in the number of tubes formed on Matrigel matrix in comparison to controls (Figure 4b,  $p < .01$ ). Of note, physiological concentrations of selenite ( $0.5 \mu\text{M}$ ) did not affect tube-like structure formation (Figure 4a,b). Indicating a role for ER stress in this response, pretreatment of cells with the chemical chaperone PBA (20 mM) restored endothelial cell tube-like structure formation ability (Figure 4a) and significantly increased the number of tubes in the PBA-treated group compared to high-selenium-treated groups (Figure 4a,b).

To harness the impact of selenium-induced ER stress on endothelial cell function, HUVECs were incubated with  $5$  and  $10 \mu\text{M}$  of selenite in the presence or absence of PERK inhibitor (GSK2606414;  $10 \mu\text{M}$ ). As depicted in Figure 5, high selenium concentrations

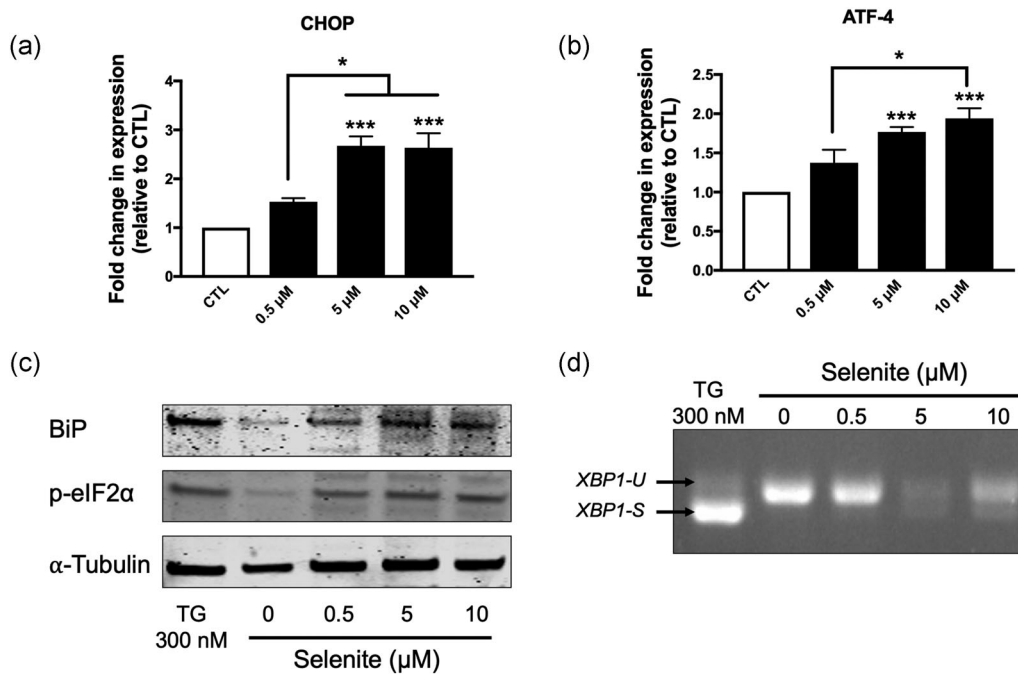


**FIGURE 2** The effects of sodium selenite on ER stress activation in endothelial cells. HUVECs were treated with sodium selenite (0, 0.5, 5, 10  $\mu\text{M}$ ) for 24 h then mRNA levels of *CHOP* (a) and *ATF-4* (b) were assessed. Results are expressed as mean  $\pm$  SEM as fold change relative to control after normalization to housekeeping gene  $\beta$ -actin mRNA expression. (c) Protein expression levels of BiP, p-eIF2 $\alpha$ , and  $\alpha$ -tubulin in HUVECs incubated with sodium selenite (0, 0.5, 5, 10  $\mu\text{M}$ ) or ER stress inducer TG (300 nM). Representative images from three independent experiments are shown. (d) *XBP-1* splicing in cells incubated with sodium selenite (0, 0.5, 5, 10  $\mu\text{M}$ ) or ER stress inducer TG (300 nM). Data analyses were done by one-way ANOVA followed with a Tukey's post hoc multiple comparison test;  $n = 5$ . ANOVA, analysis of variance; ATF-4, activating transcription factor 4; CHOP, C/EBP homologous protein; ER, endoplasmic reticulum; HUVEC, human umbilical vein endothelial cell; TG, thapsigargin. \* $p < .05$ , \*\*\* $p < .001$  versus untreated group (CTL) or versus indicated group

decreased the ability of cells to organize in tubes; however, the pre-incubation of cells with the PERK inhibitor significantly prevented the effects of high selenium concentrations, showing a significant increase in tube-like structure formation from two and one tubes to 21 and 19 tubes ( $p < .05$ ), respectively (Figure 5a,b). These data

corroborate the observations with the chemical chaperone PBA (Figure 4).

As endothelial function depends on NO production and bioavailability, which can be affected by ROS, we measured NO and ROS levels after sodium selenite treatment (Figure 6). As shown in

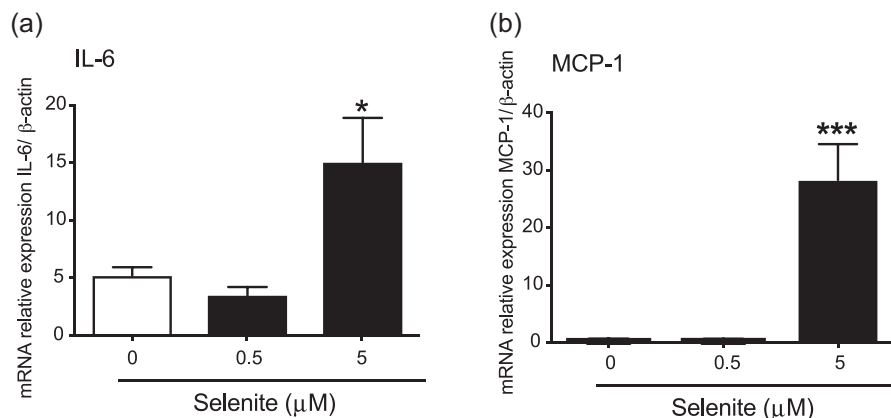


**FIGURE 3** The effects of sodium selenite on mRNA expression of inflammatory genes in endothelial cells. HUVECs were incubated with sodium selenite (0, 0.5, 5  $\mu\text{M}$ ) for 8 h, and then mRNA expression of *IL-6* (a) and *MCP-1* (b) was assessed. Results are presented as mean  $\pm$  SEM as relative expression normalized to the housekeeping gene  $\beta$ -actin. Analyses were done by one-way ANOVA followed with a Tukey's post hoc multiple comparison test;  $n = 5$ . ANOVA, analysis of variance; HUVEC, human umbilical vein endothelial cell; IL-6, interleukin-6; MCP-1, monocyte chemoattractant protein-1; mRNA, messenger RNA. \* $p < .05$ , \*\*\* $p < .001$  versus untreated group (CTL) and 0.5  $\mu\text{M}$  condition

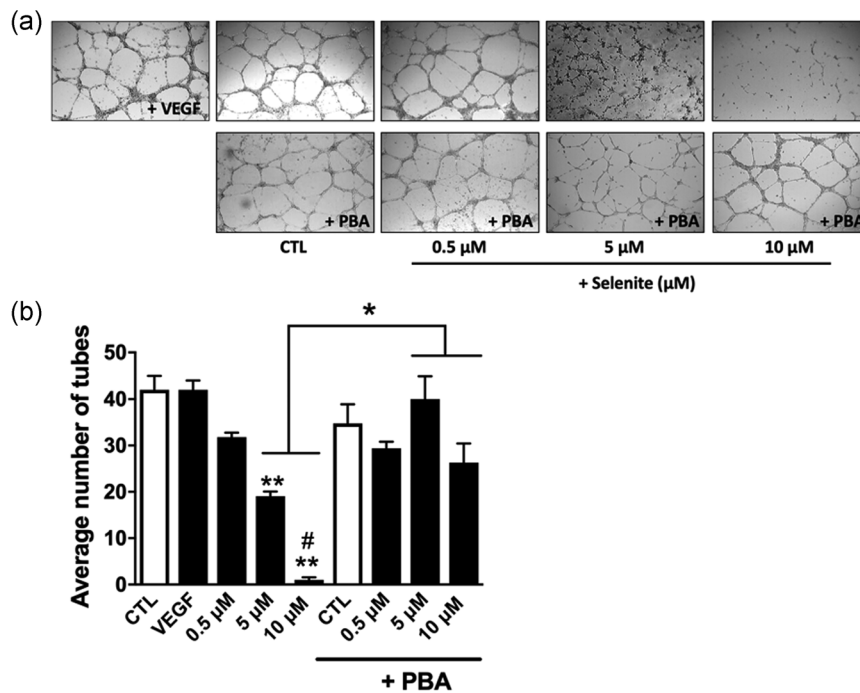


**FIGURE 4** The effects of sodium selenite on endothelial angiogenic capacity. (a) Pictures of HUVEC cells cultured in complete M200 medium (containing LSGS) and supplemented with VEGF (positive control), in M200 nonsupplemented with LSGS (negative control or CTL or no selenite), or in complete M200 containing sodium selenite (0.5, 5, 10  $\mu\text{M}$ ) in combination or not with PBA (20 mM). HUVECs were then seeded on Matrigel to encourage tube formation. Representative images are shown from three independent assays (captured after 6 h;  $\times 100$  magnification). To quantify angiogenesis, the number of tubes formed was counted in five random fields for each well using ImageJ software. (b) Bars represent the pooled data expressed as the average number of tubes formed in each condition. Results are expressed as mean  $\pm$  SEM and analyses were done by one-way ANOVA, followed with a Tukey's post hoc multiple comparison test;  $n = 3$ . ANOVA, analysis of variance; HUVEC, human umbilical vein endothelial cell; LSGS, low serum growth supplement; PBA, sodium 4-phenylbutyrate; VEGF, vascular endothelial growth factor. \* $p < .05$ , \*\* $p < .01$  versus negative control (CTL) or indicated groups; # $p < .05$  versus selenite 0.5  $\mu\text{M}$  group

Figure 6a,b, high selenite concentrations (5 and 10  $\mu\text{M}$ ) dramatically increased the proportion of cells positive for DHE staining compared to the physiological concentration of selenite (0.5  $\mu\text{M}$ ) and controls ( $p < .001$ ). Hydrogen peroxide ( $\text{H}_2\text{O}_2$ ) was used as a positive control in this experiment. The pre-incubation of cells with PBA significantly prevented ROS production, which was reduced from 69% and 68% to 23.5% and 18.6% in cells incubated with 5 and 10  $\mu\text{M}$  of selenite, respectively (Figure 6a,b), further implicating ER stress. Figure 6c shows that incubation of cells with high selenite concentrations (5 and 10  $\mu\text{M}$ ) reduced the production of NO, as shown by the significant reduction in nitrite concentrations in culture media compared to control and low selenium concentration (0.5  $\mu\text{M}$ ) conditions. The pre-incubation of cells with PBA (20 mM) prevented the effects of high selenite concentration on NO production (Figure 6c). This concomitant reduction in NO release and increase in ROS production by high selenite concentration contributes to the decrease in NO bioavailability.

The interaction between eNOS and caveolin-1 is critical for the activity of eNOS. When eNOS interacts with caveolin-1, eNOS is maintained in an inactive state and calmodulin requires to allosterically compete with caveolin-1 to cause calcium-dependent activation of eNOS, and hence high expression levels of caveolin-1 may reduce the activation of eNOS (Feron & Balligand, 2006). Therefore,

we investigated the mRNA expression of *caveolin-1* in endothelial cells exposed to physiological and high concentrations of selenite. Interestingly, the physiological concentration of selenite (0.5  $\mu\text{M}$ ) decreased the mRNA expression of *caveolin-1* that is known for sequestering eNOS in caveolae and, hence preventing its activation. However, a high concentration of selenite (5  $\mu\text{M}$ ) significantly increased the mRNA expression of *caveolin-1* compared to the control and low selenite concentration ( $p < .01$ ) as shown in Figure 6d.

Altogether, our results suggest that high selenite concentrations decreased NO bioavailability by reducing NO production, coupled to increased ROS, in a mechanism involving ER stress. Combined, these effects contributed to impairment of endothelial function as evidenced by a reduced capacity to form a tube-like structure on a Matrigel assay (Figures 4 and 5).

### 3.4 | High selenite concentrations caused endothelial-cell dysfunction via a process involving ER stress-induced cell death

To further investigate the mechanism behind the effects induced by sodium selenite, an evaluation of cell death was undertaken. Treatment with high selenite concentrations, 5 and 10  $\mu\text{M}$ , led to 36.8%

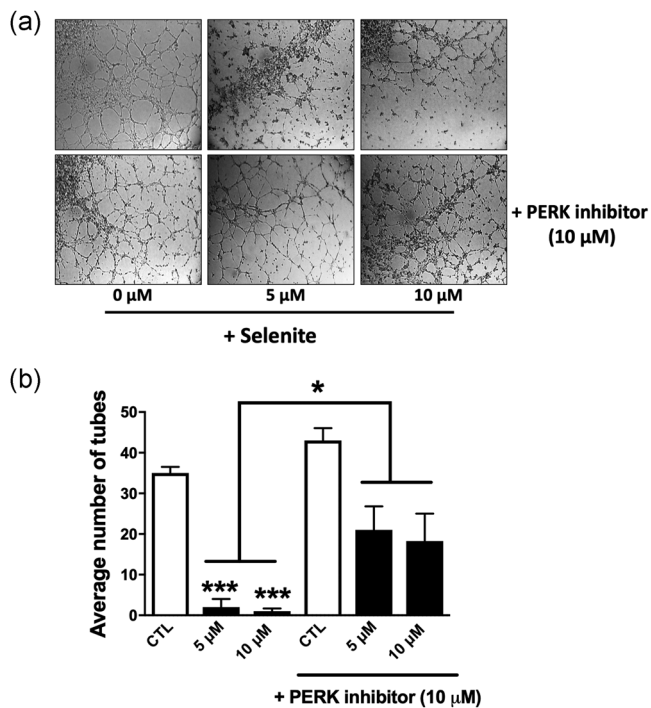


**FIGURE 5** The impact of PERK inhibition on the actions of sodium selenite on endothelial angiogenic capacity. (a) Pictures of HUVEC cells cultured in M200 non-supplemented with LSGS (negative control or CTL or no selenite) or in complete M200 containing sodium selenite (0.5, 5, 10 μM) in combination or not with PERK inhibitor (GSK2606414, 10 μM). Cells were then seeded on a Matrigel to encourage tube-like structure formation. Images shown are representative of three independent assays (captured after 6 h; ×40 magnification). To quantify angiogenesis, the number of tubes formed was counted in five random fields for each well using ImageJ software. (b) Bars represent the pooled data expressed as the average number of tubes formed in each condition. Results are expressed as mean ± SEM and analyses were done by one-way ANOVA, followed with Tukey's post hoc multiple comparison test;  $n = 3$ . ANOVA, analysis of variance; LSGS, low serum growth supplement; PERK, protein kinase RNA-like endoplasmic reticulum kinase. \* $p < .05$ ; \*\*\* $p < .001$  versus negative control (CTL) or indicated groups

and 43.7% apoptosis, respectively, compared to controls and physiological concentration of selenite (0.5 μM; Figure 7a,b). Pretreatment with PBA significantly protected cells from apoptosis induced by high selenite concentrations ( $p < .01$ ; Figure 7a,b), demonstrating the implication of the ER stress response in this phenomenon.

Next, we assessed the specific apoptotic sub-pathway involved in cell death induced by high selenite. As shown in Figure 7c,d, a significant increase in the activity of caspases 3 and 7—by 2-fold ( $p < .001$ ) and 1.5-fold ( $p < .01$ )—was observed in endothelial cells treated with a high concentration of selenite (5 μM) after 8 and 24 h of incubation, respectively, compared to untreated cells and those treated with a physiological concentration of selenite (0.5 μM). The pretreatment of cells with PBA prevented the activation of caspases 3 and 7 in cells treated with 5 μM selenite (Figure 7c,d). Altogether,

these data indicate that high selenite concentrations caused an increase in cell death mediated by ER stress in a mechanism involving the activation of caspases 3 and 7.

## 4 | DISCUSSION

High selenium intake has been associated with insulin resistance, thus it may increase the risk of type-2 diabetes (Bleys et al., 2007; Rayman, 2012; Stranges et al., 2007). Furthermore, insulin resistance has been shown to contribute to endothelial dysfunction thereby increasing the risk of cardiovascular disease (Abdelsalam et al., 2019; Kim et al., 2006; H. Wang et al., 2013). Here, we investigated the impact of high selenium, as sodium selenite, on endothelial cell function and the molecular mechanisms involved with a special focus on the implication of oxidative stress and ER-stress response.

We report here for the first time, that in contrast to a physiological concentration of sodium selenite, supra-physiological concentrations induced both oxidative stress and the ER stress in endothelial cells in vitro. These selenium-mediated stress responses resulted in reduced NO bioavailability and endothelial dysfunction characterized by impaired angiogenic capacity in a mechanism involving ER-stress-mediated apoptosis. Our results therefore clearly indicate that exposure to high selenium, like selenite, causes endothelial cell dysfunction, a critical feature of atherosclerosis, a condition that precedes cardiovascular disease.

Our study supports previous findings that ER stress is associated with endothelial dysfunction. Our findings are in line with previous studies that have demonstrated a key role for ER stress in endothelial-cell inflammation, dysfunction, and apoptosis (Chen et al., 2012). We also extend this observation by reporting, for the first time, that high selenium induces the expression of several key markers of ER stress both at the mRNA and protein levels in endothelial cells, in a time- and dose-dependent manner. Additionally, we found that high selenium leads to endothelial cell dysfunction via the induction of oxidative stress in a close interplay with ER stress. There is much evidence in the literature indicating a crosstalk between ER stress and oxidative stress suggesting that ER stress and oxidative stress can be induced by one another in a vicious circle. In endothelial cells, an increase in ROS as  $O_2^-$  leads to rapid interaction with NO to form a more reactive free radical, peroxynitrite, that results in reduced bioavailability of NO and thus contributes to impairment of endothelial function (Gage et al., 2013). Furthermore, impaired bioavailability of NO leads to impaired NO-mediated angiogenesis (Maamoun et al., 2017). Our results indicate that high selenium, in the form of sodium selenite, causes endothelial dysfunction by reducing NO bioavailability as a result of the concomitant release of ROS and reduced NO production. Reduction in NO bioavailability eventually contributes to the impaired angiogenic capacity observed as shown by the tube-like formation assay in a mechanism involving ER-stress activation.

Endothelial cell apoptosis is associated with impaired angiogenic capacity (Maamoun, Abdelsalam, et al., 2019). Our novel findings



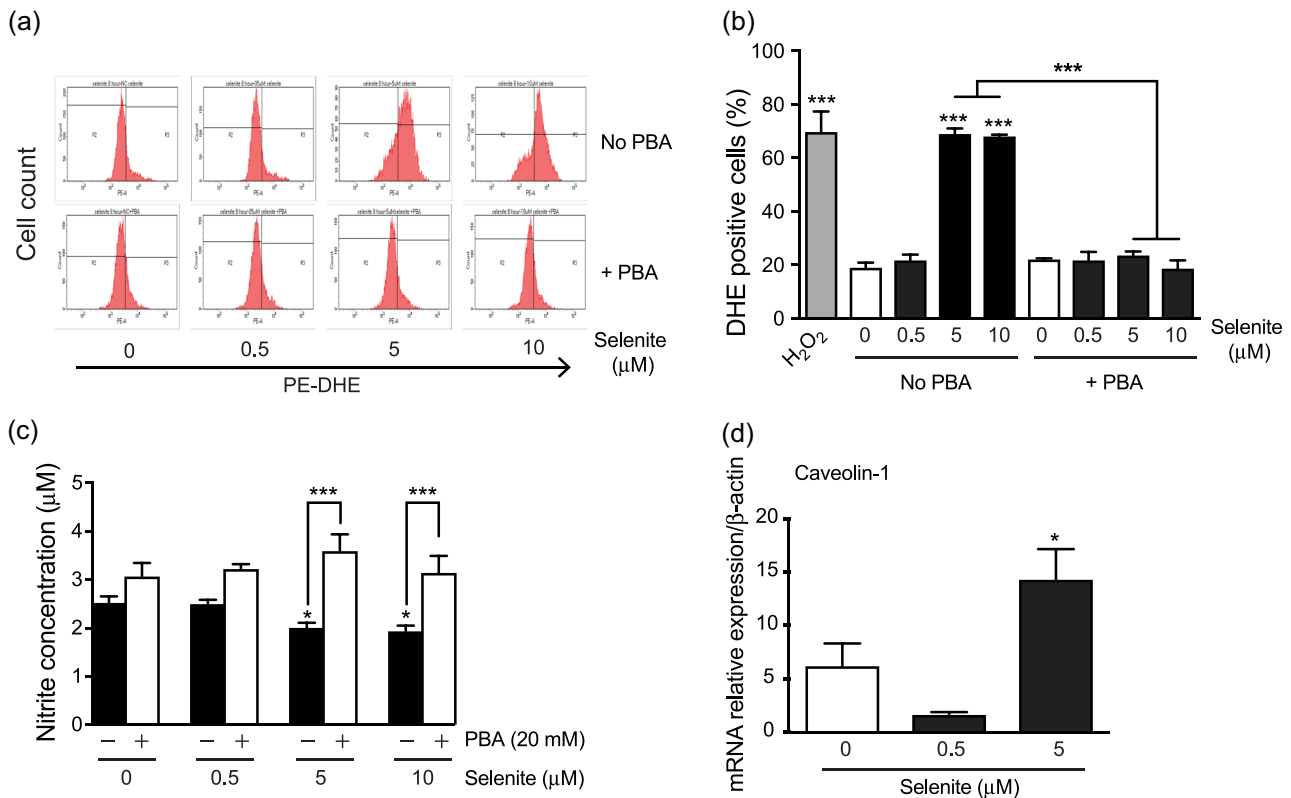


**FIGURE 6** Effects of sodium selenite on ROS and NO production. (a,b) Assessment of ROS release in EA.hy926 cells. Cells were incubated in culture medium supplemented for 24 h with sodium selenite (0, 0.5, 5, 10 µM) in combination or not with PBA (20 mM) or with H<sub>2</sub>O<sub>2</sub> (100 µM; 30 min), acting as a positive control. (a) shows representative flow cytometry images. Bars (b) indicate the proportion of cells positive for DHE staining relative to the untreated group. (c) Nitrite concentrations in EA.hy926 cells. Cells were treated with sodium selenite (0, 0.5, 5, 10 µM) for 24 h in combination or not with PBA (20 mM). Supernatants were then harvested, and nitrite levels were assayed using the Griess reagent assay. (d) *Caveolin-1* mRNA expression in HUVECs incubated with sodium selenite (0, 0.5, 5 µM) for 8 h. Bars represent relative mRNA expression normalized to housekeeping gene  $\beta$ -actin. Results are presented as mean  $\pm$  SEM and analyses were done by one-way ANOVA followed with a Tukey's post hoc multiple comparison test;  $n = 5$ . ANOVA, analysis of variance; HUVEC, human umbilical vein endothelial cell; mRNA, messenger RNA; PBA, sodium 4-phenylbutyrate; ROS, reactive oxygen species. \*  $p < .05$ , \*\*\* $p < .001$  versus untreated group (CTL) and selenite 0.5 µM group or indicated groups

report that high selenium concentrations, unlike physiological concentrations, induced apoptosis in endothelial cells in a mechanism that involves the activation of ER stress and downstream caspases 3 and 7. Although no previous studies have investigated the impact of high selenium on endothelial cell death, several cancer studies indicated the implication of ER stress in the cytotoxicity induced by high selenite in carcinoma cell lines (Suzuki et al., 2010), and in promyelocytic leukemia cells (Guan et al., 2009). Endothelial cell apoptosis is a key contributor to the dysfunction of endothelial cells. We reported previously that high glucose growth conditions induced ER-stress-mediated apoptosis that was associated with oxidative stress and reduced angiogenic capacity in endothelial cells (Maamoun et al., 2017).

Selenium supplementation is now increasingly accepted as a promising adjuvant therapy in radiation oncology due to its cytoprotective effects (Muecke et al., 2018) and also in cancer therapy for various types of cancers due to its anticancer properties (Pang & Chin, 2019). Selenium is reported to display key anti-neoplastic properties both in vivo and in vitro. Inorganic and organic selenium

are able to cause cell cycle arrest, and apoptosis in multiple cancer cell lines such as colon, breast, lung, and prostate. High levels, however, of inorganic and organic selenium are required to enhance oxidative stress in cancer cells and mediate these anticancer properties. Considering our finding that endothelial dysfunction is driven by ER stress induced by high selenium, it might be anticipated that those cancer patients supplemented with high dose selenium would have an increased risk of cardiovascular diseases. Selenium is critical for many physiological processes and an adequate intake and status are very important for human health. However, the status and intake around the world are very variable from one region to another with some regions/countries sufficient, others insufficient, and some over-sufficient. Given its vital roles for health, the consumption of selenium-containing supplements, readily available over the counter, is rising which may predispose individuals to an excess of selenium intake and lead to potential adverse effects (Rayman, 2020). Our findings here strengthen the notion that while appropriate selenium intake is beneficial for health, its excess may be associated with the activation of

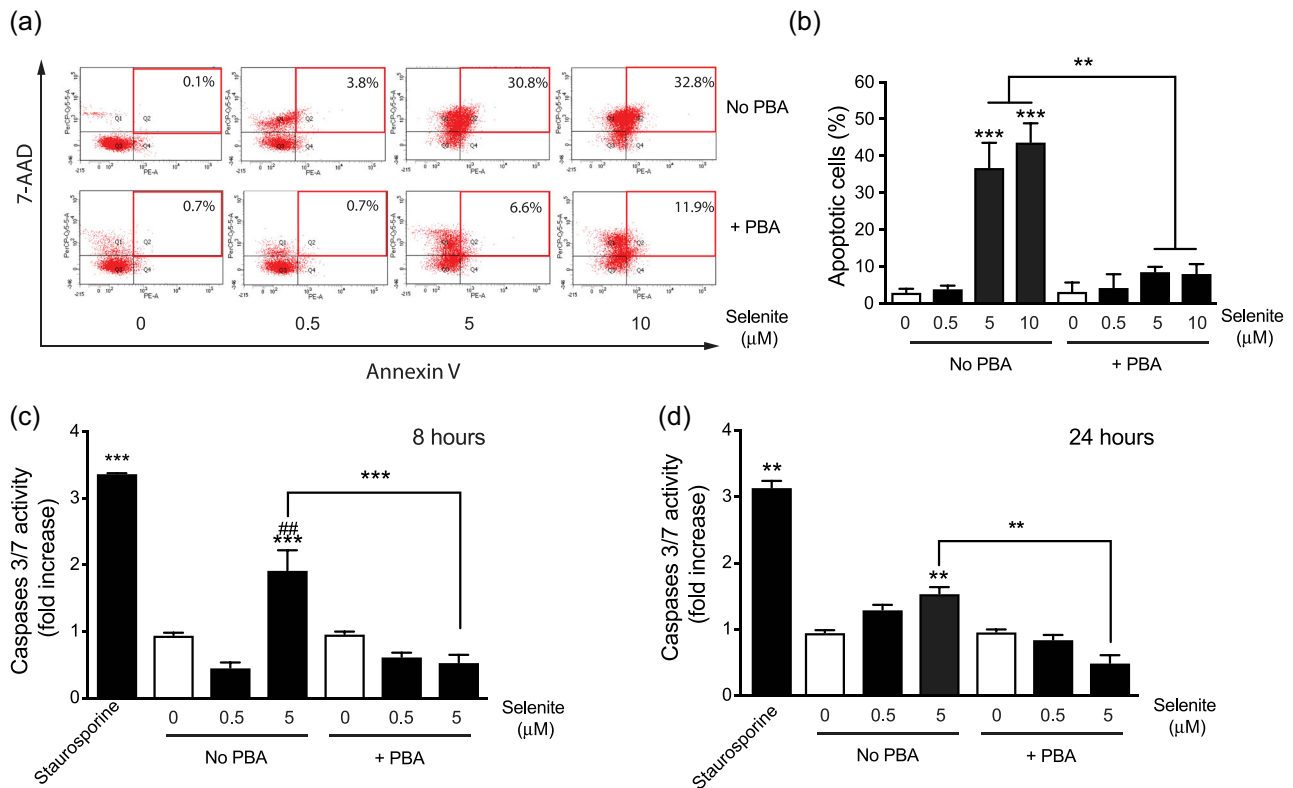


**FIGURE 7** Effects of sodium selenite on apoptosis in endothelial cells. (a,b) Measurement of cell death by flow cytometry in EA.hy926 cells. Cells were incubated in culture medium supplemented for 24 h with sodium selenite (0, 0.5, 5, 10 μM) in combination or not with PBA (20 mM). (a) Shows representative flow cytometry images. (b) Bars represent the percentage of apoptotic cells. Results are expressed as mean ± SEM and analyses were done by two-way ANOVA followed with a Tukey's post hoc multiple comparison test.  $n = 4-7$ ;  $**p < .01$ ,  $***p < .001$  versus untreated group (CTL) and selenite 0.5 μM group or indicated groups. (c,d) Caspase 3 and 7 activity luminescent assay. A positive control was derived from cells treated with staurosporine (1 μM, 3 h). EA.hy926 cells were incubated in a medium supplemented with sodium selenite (0, 0.5, 5 μM) for 8 h (c) or 24 h (d) in combination or not with PBA (20 mM). Data are presented as mean ± SEM and analyses were done by one-way ANOVA followed with a Tukey's post hoc multiple comparison test;  $n = 3$ . ANOVA, analysis of variance; PBA, sodium 4-phenylbutyrate.  $**p < .01$ ,  $***p < .001$  versus untreated group (CTL) or versus indicated groups;  $##p < .01$  versus selenite 0.5 μM group

deleterious cellular and molecular pathways that can contribute to an increased risk of cardiovascular complications. Therefore, it is essential to underscore the importance of optimal and balanced supplementation of selenium to prevent any non-desirable adverse effects. However, the main limitation of our study is that it was conducted in vitro in cultured cells and results need to be further confirmed in a whole-body system in vivo using animal models such as rodents receiving a diet supplemented with various levels of selenium to ascertain their translational aspect.

In conclusion, we showed here that high-selenium concentrations caused endothelial dysfunction via a mechanism involving cell death mediated by ER stress. These findings point to the importance of appropriate intake or supplementation of selenium to optimize health benefits. These results also underscore the relevance of monitoring the risk of cardiovascular disease in cancer patients who are being supplemented with selenium as part of their chemotherapeutic intervention or during radiotherapy. This study also suggests that the uncontrolled use of selenium supplements as a prophylactic agent against oxidative stress may entail risk.

#### ACKNOWLEDGMENTS

Our work is supported by research grants from the Royal Society (RG120480), Qatar University (QUCG-CPH-20/21-3) and the Qatar National Research Fund (UREP24-016-3-004) to Dr. Abdelali Agouni. M. Zachariah and H. Maamoun were supported by doctoral (PhD) scholarships from the University of Botswana and the Egyptian cultural bureau, respectively. L. Milano was supported by a Science without Borders studentship (CNPq - Brazil). The graphical abstract was partly generated by using freely licensed tools from Servier Medical Art (SMART), available under a Creative Commons Attribution 3.0 Unported License <https://creativecommons.org/licenses/by/3.0/>. Open Access funding provided by the Qatar National Library.

#### CONFLICT OF INTERESTS

The authors declare that there are no conflicts of interests.

#### AUTHOR CONTRIBUTIONS

Abdelali Agouni and Margaret P. Rayman conceptualized the research study idea. Abdelali Agouni and Lisiane B. Meira designed the

research plan. Abdelali Agouni acquired the funding. Abdelali Agouni and Lisiane B. Meira supervised the experiments and curated the data. Matshediso Zachariah, Hatem Maamoun, and Larissa Milano performed the experiments and collected data. All authors contributed to the analysis of data. Matshediso Zachariah, Abdelali Agouni, and Lisiane B. Meira wrote the manuscript and prepared the figures with input from all authors.

## DATA AVAILABILITY STATEMENT

The data supporting the conclusions of this study are available from the corresponding author upon reasonable request.

## ORCID

Abdelali Agouni  <http://orcid.org/0000-0002-8363-1582>

## REFERENCES

- Abdelsalam, S. S., Korashy, H. M., Zeidan, A., & Agouni, A. (2019). The role of protein tyrosine phosphatase (PTP)-1B in cardiovascular disease and its interplay with insulin resistance. *Biomolecules*, *9*(7), 286. <https://doi.org/10.3390/biom9070286>
- Agouni, A., Mody, N., Owen, C., Czopek, A., Zimmer, D., Bentires-Alj, M., Bence, K. K., & Delibegović, M. (2011). Liver-specific deletion of protein tyrosine phosphatase (PTP) 1B improves obesity- and pharmacologically induced endoplasmic reticulum stress. *Biochemical Journal*, *438*(2), 369–378. <https://doi.org/10.1042/BJ20110373>
- Bleys, J., Navas-Acien, A., & Guallar, E. (2007). Serum selenium and diabetes in U.S. adults. *Diabetes Care*, *30*(4), 829–834. <https://doi.org/10.2337/dc06-1726>
- Bleys, J., Navas-Acien, A., & Guallar, E. (2008). Serum selenium levels and all-cause, cancer, and cardiovascular mortality among US adults. *Archives of Internal Medicine*, *168*(4), 404–410. <https://doi.org/10.1001/archinternmed.2007.74>
- Bleys, J., Navas-Acien, A., Stranges, S., Menke, A., Miller, E. R., & Guallar, E. (2008). Serum selenium and serum lipids in US adults. *American Journal of Clinical Nutrition*, *88*(2), 416–423.
- Burk, R. F. (2002). Selenium, an antioxidant nutrient. *Nutrition in Clinical Care*, *5*(2), 75–79. <https://doi.org/10.1046/j.1523-5408.2002.00006.x>
- Burk, R. F., & Hill, K. E. (2015). Regulation of selenium metabolism and transport. *Annual Review of Nutrition*, *35*(1), 150514143029003. <https://doi.org/10.1146/annurev-nutr-071714-034250>
- Chen, Y., Wang, J. J., Li, J., Hosoya, K. I., Ratan, R., Townes, T., & Zhang, S. X. (2012). Activating transcription factor 4 mediates hyperglycaemia-induced endothelial inflammation and retinal vascular leakage through activation of STAT3 in a mouse model of type 1 diabetes. *Diabetologia*, *55*(9), 2533–2545. <https://doi.org/10.1007/s00125-012-2594-1>
- Choi, S. K., Lim, M., Byeon, S. H., & Lee, Y. H. (2016). Inhibition of endoplasmic reticulum stress improves coronary artery function in the spontaneously hypertensive rats. *Scientific Reports*, *6*, 31925. <https://doi.org/10.1038/srep31925>
- Cnop, M., Foufelle, F., & Velloso, L. A. (2012). Endoplasmic reticulum stress, obesity and diabetes. *Trends in Molecular Medicine*, *18*(1), 59–68. <https://doi.org/10.1016/j.molmed.2011.07.010>
- Cunningham, K. S., & Gotlieb, A. I. (2005). The role of shear stress in the pathogenesis of atherosclerosis. *Laboratory Investigation*, *85*, 9–23. <https://doi.org/10.1038/labinvest.3700215>
- Delibegovic, M., Zimmer, D., Kauffman, C., Rak, K., Hong, E. G., Cho, Y. R., Kim, J. K., Kahn, B. B., Neel, B. G., & Bence, K. K. (2009). Liver-specific deletion of protein-tyrosine phosphatase 1B (PTP1B) improves metabolic syndrome and attenuates diet-induced endoplasmic reticulum stress. *Diabetes*, *58*(3), 590–599. <https://doi.org/10.2337/db08-0913>
- Dinh, Q. N., Drummond, G. R., Sobey, C. G., & Chrissobolis, S. (2014). Roles of inflammation, oxidative stress, and vascular dysfunction in hypertension. *BioMed Research International*, *2014*, 406960. <https://doi.org/10.1155/2014/406960>
- Feron, O., & Balligand, J. L. (2006). Caveolins and the regulation of endothelial nitric oxide synthase in the heart. *Cardiovascular Research*, *69*(4), 788–797. <https://doi.org/10.1016/j.cardiores.2005.12.014>
- Gage, M. C., Yuldasheva, N. Y., Viswambharan, H., Sukumar, P., Cubbon, R. M., Galloway, S., Imrie, H., Skromna, A., Smith, J., Jackson, C. L., Kearney, M. T., & Wheatcroft, S. B. (2013). Endothelium-specific insulin resistance leads to accelerated atherosclerosis in areas with disturbed flow patterns: A role for reactive oxygen species. *Atherosclerosis*, *230*(1), 131–139. <https://doi.org/10.1016/j.atherosclerosis.2013.06.017>
- Galan, M., Kassan, M., Choi, S. K., Partyka, M., Trebak, M., Henrion, D., & Matrougui, K. (2012). A novel role for epidermal growth factor receptor tyrosine kinase and its downstream endoplasmic reticulum stress in cardiac damage and microvascular dysfunction in type 1 diabetes mellitus. *Hypertension*, *60*(1), 71–80. <https://doi.org/10.1161/HYPERTENSIONAHA.112.192500>
- Galán, M., Kassan, M., Kadowitz, P. J., Trebak, M., Belmadani, S., & Matrougui, K. (2014). Mechanism of endoplasmic reticulum stress-induced vascular endothelial dysfunction. *Biochimica et Biophysica Acta—Molecular Cell Research*, *1843*(6), 1063–1075. <https://doi.org/10.1016/j.bbamcr.2014.02.009>
- Guan, L., Han, B., Li, Z., Hua, F., Huang, F., Wei, W., Yang, Y., & Xu, C. (2009). Sodium selenite induces apoptosis by ROS-mediated endoplasmic reticulum stress and mitochondrial dysfunction in human acute promyelocytic leukemia NB4 cells. *Apoptosis*, *14*(2), 218–225. <https://doi.org/10.1007/s10495-008-0295-5>
- Hermann, M., Flammer, A., & Lscher, T. F. (2006). Nitric oxide in hypertension. *The Journal of Clinical Hypertension*, *8*(12 Suppl. 4), 17–29. <https://doi.org/10.1111/j.1524-6175.2006.06032.x>
- Hetz, C. (2012). The unfolded protein response: Controlling cell fate decisions under ER stress and beyond. *Nature Reviews Molecular Cell Biology*, *13*(2), 89–102. <https://doi.org/10.1038/nrm3270>
- Ibrahim, S. A. Z., Kerkadi, A., & Agouni, A. (2019). Selenium and health: An update on the situation in the Middle East and North Africa. *Nutrients*, *11*(7), 1457. <https://doi.org/10.3390/nu11071457>
- Incalza, M. A., D'Oria, R., Naticichio, A., Perrini, S., Laviola, L., & Giorgino, F. (2018). Oxidative stress and reactive oxygen species in endothelial dysfunction associated with cardiovascular and metabolic diseases. *Vascular Pharmacology*, *100*, 1–19. <https://doi.org/10.1016/j.vph.2017.05.005>
- Ip, C. (1998). Lessons from basic research in selenium and cancer prevention. *Journal of Nutrition*, *128*(11), 1845–1854. <https://doi.org/10.1093/jn/128.11.1845>
- Kim, J. A., Montagnani, M., Koh, K. K., & Quon, M. J. (2006). Reciprocal relationships between insulin resistance and endothelial dysfunction: Molecular and pathophysiological mechanisms. *Circulation*, *113*(15), 1888–1904. <https://doi.org/10.1161/CIRCULATIONAHA.105.563213>
- Labunskyy, V. M., Lee, B. C., Handy, D. E., Loscalzo, J., Hatfield, D. L., & Gladyshev, V. N. (2011). Both maximal expression of selenoproteins and selenoprotein deficiency can promote development of type 2 diabetes-like phenotype in mice. *Antioxidants & Redox Signaling*, *14*(12), 2327–2336. <https://doi.org/10.1089/ars.2010.3526>
- Lenna, S., Han, R., & Trojanowska, M. (2014). Endoplasmic reticulum stress and endothelial dysfunction. *IUBMB Life*, *66*, 530–537.
- Levick, J. R. (2003). *An introduction to cardiovascular physiology* (4th ed.). Arnold.

- Maamoun, H., Abdelsalam, S. S., Zeidan, A., Korashy, H. M., & Agouni, A. (2019). Endoplasmic reticulum stress: A critical molecular driver of endothelial dysfunction and cardiovascular disturbances associated with diabetes. *International Journal of Molecular Sciences*, 20(7), 1658. <https://doi.org/10.3390/ijms20071658>
- Maamoun, H., Benameur, T., Pintus, G., Munusamy, S., & Agouni, A. (2019). Crosstalk between oxidative stress and endoplasmic reticulum (ER) stress in endothelial dysfunction and aberrant angiogenesis associated with diabetes: A focus on the protective roles of heme oxygenase (HO)-1. *Frontiers in Physiology*, 10, 70. <https://doi.org/10.3389/fphys.2019.00070>
- Maamoun, H., Zachariah, M., McVey, J. H., Green, F. R., & Agouni, A. (2017). Heme oxygenase (HO)-1 induction prevents endoplasmic reticulum stress-mediated endothelial cell death and impaired angiogenic capacity. *Biochemical Pharmacology*, 127, 46–59. <https://doi.org/10.1016/j.bcp.2016.12.009>
- Mostefai, H. A., Agouni, A., Carusio, N., Mastronardi, M. L., Heymes, C., Henrion, D., Andriantsitohaina, R., & Martinez, M. C. (2008). Phosphatidylinositol 3-kinase and xanthine oxidase regulate nitric oxide and reactive oxygen species productions by apoptotic lymphocyte microparticles in endothelial cells. *Journal of Immunology*, 180(7), 5028–5035. <https://doi.org/10.4049/jimmunol.180.7.5028>
- Muecke, R., Micke, O., Schomburg, L., Buentzel, J., Kisters, K., Adamietz, I. A., & Akte (2018). Selenium in radiation oncology—15 years of experiences in Germany. *Nutrients*, 10(4), <https://doi.org/10.3390/nu10040483>
- Ozcan, U., Cao, Q., Yilmaz, E., Lee, A.-H., Iwakoshi, N. N., Ozdelen, E., Tuncman, G., Görgün, C., Glimcher, L. H., & Hotamisligil, G. S. (2004). Endoplasmic reticulum stress links obesity, insulin action, and type 2 diabetes. *Science*, 306(5695), 457–461. <https://doi.org/10.1126/science.1103160>
- Pang, K. L., & Chin, K. Y. (2019). Emerging anticancer potentials of selenium on osteosarcoma. *International Journal of Molecular Sciences*, 20(21), <https://doi.org/10.3390/ijms20215318>
- Pennathur, S., & Heinecke, J. W. (2007). Oxidative stress and endothelial dysfunction in vascular disease. *Current Diabetes Reports*, 7(4), 257–264. <https://doi.org/10.1007/s11892-007-0041-3>
- Pillai, R., Uyehara-Lock, J. H., & Bellinger, F. P. (2014). Selenium and selenoprotein function in brain disorders. *IUBMB Life*, 66, 229–239.
- Rayman, M. P. (2012). Selenium and human health. *Lancet*, 379(9822), 1256–1268. [https://doi.org/10.1016/S0140-6736\(11\)61452-9](https://doi.org/10.1016/S0140-6736(11)61452-9)
- Rayman, M. P. (2020). Selenium intake, status, and health: A complex relationship. *Hormones*, 19(1), 9–14. <https://doi.org/10.1007/s42000-019-00125-5>
- Rocourt, C. R. B., & Cheng, W. H. (2013). Selenium supranutrition: Are the potential benefits of chemoprevention outweighed by the promotion of diabetes and insulin resistance? *Nutrients*, 5(4), 1349–1365.
- Schroder, M., & Kaufman, R. J. (2005). ER stress and the unfolded protein response. *Mutation Research/DNA Repairs*, 569(1-2), 29–63. <https://doi.org/10.1016/j.mrfmmm.2004.06.056>
- Schwarz, D. S., & Blower, M. D. (2016). The endoplasmic reticulum: Structure, function and response to cellular signaling. *Cellular and Molecular Life Science*, 73(1), 79–94. <https://doi.org/10.1007/s00018-015-2052-6>
- Selenius, M., Rundlof, A. K., Olm, E., Fernandes, A. P., & Bjornstedt, M. (2010). Selenium and the selenoprotein thioredoxin reductase in the prevention, treatment and diagnostics of cancer. *Antioxidants & Redox Signaling*, 12(7), 867–880. <https://doi.org/10.1089/ars.2009.2884>
- Sozen, E., Karademir, B., & Ozer, N. K. (2015). Basic mechanisms in endoplasmic reticulum stress and relation to cardiovascular diseases. *Free Radical Biology and Medicine*, 78, 30–41. <https://doi.org/10.1016/j.freeradbiomed.2014.09.031>
- Steinbrenner, H., Speckmann, B., Pinto, A., & Sies, H. (2011). High selenium intake and increased diabetes risk: Experimental evidence for interplay between selenium and carbohydrate metabolism. *Journal of Clinical Biochemistry and Nutrition*, 48, 40–45.
- Stranges, S., Marshall, J. R., Natarajan, R., Donahue, R. P., & Trevisan, M. (2007). Effects of long-term selenium supplementation on the incidence of type 2 diabetes: A randomized trial. *Annals of Internal Medicine*, 147(4), 217–224.
- Suzuki, M., Endo, M., Shinohara, F., Echigo, S., & Rikiishi, H. (2010). Differential apoptotic response of human cancer cells to organoselenium compounds. *Cancer Chemotherapy and Pharmacology*, 66(3), 475–484. <https://doi.org/10.1007/s00280-009-1183-6>
- Wang, H., Wang, A. X., Aylor, K., & Barrett, E. J. (2013). Nitric oxide directly promotes vascular endothelial insulin transport. *Diabetes*, 62(12), 4030–4042. <https://doi.org/10.2337/db13-0311>
- Wang, M., & Kaufman, R. J. (2014). The impact of the endoplasmic reticulum protein-folding environment on cancer development. *Nature Reviews Cancer*, 14(9), 581–597. <https://doi.org/10.1038/nrc3800>
- Werstuck, G. H., Khan, M. I., Femia, G., Kim, A. J., Tedesco, V., Trigatti, B., & Shi, Y. (2006). Glucosamine-induced endoplasmic reticulum dysfunction is associated with accelerated atherosclerosis in a hyperglycemic mouse model. *Diabetes*, 55(1), 93–101. <https://www.ncbi.nlm.nih.gov/pubmed/16380481>
- Werstuck, G. H., Lentz, S. R., Dayal, S., Hossain, G. S., Sood, S. K., Shi, Y. Y., Zhou, J., Maeda, N., Krisans, S. K., Malinow, M. R., & Austin, R. C. (2001). Homocysteine-induced endoplasmic reticulum stress causes dysregulation of the cholesterol and triglyceride biosynthetic pathways. *Journal of Clinical Investigation*, 107(10), 1263–1273. <https://doi.org/10.1172/JCI11596>
- WHO. (2017). World Health Statistics 2017: Monitoring Health for The SDGs.
- Wu, Y., Zhang, H., Dong, Y., Park, Y. M., & Ip, C. (2005). Endoplasmic reticulum stress signal mediators are targets of selenium action. *Cancer Research*, 65(19), 9073–9079. <https://doi.org/10.1158/0008-5472.CAN-05-2016>
- Xiang, N., Zhao, R., & Zhong, W. (2009). Sodium selenite induces apoptosis by generation of superoxide via the mitochondrial-dependent pathway in human prostate cancer cells. *Cancer Chemotherapy and Pharmacology*, 63(2), 351–362. <https://doi.org/10.1007/s00280-008-0745-3>
- Yoshida, H., Matsui, T., Yamamoto, A., Okada, T., & Mori, K. (2001). XBP1 mRNA is induced by ATF6 and spliced by IRE1 in response to ER stress to produce a highly active transcription factor. *Cell*, 107(7), 881–891. [https://doi.org/10.1016/S0092-8674\(01\)00611-0](https://doi.org/10.1016/S0092-8674(01)00611-0)
- Zhou, J., Lhotak, S., Hilditch, B. A., & Austin, R. C. (2005). Activation of the unfolded protein response occurs at all stages of atherosclerotic lesion development in apolipoprotein E-deficient mice. *Circulation*, 111(14), 1814–1821. <https://doi.org/10.1161/01.CIR.0000160864.31351.C1>

**How to cite this article:** Zachariah M, Maamoun H, Milano L, Rayman MP, Meira LB, Agouni A. Endoplasmic reticulum stress and oxidative stress drive endothelial dysfunction induced by high selenium. *J Cell Physiol*. 2020;1–12. <https://doi.org/10.1002/jcp.30175>